Research in Pharmaceutical Sciences, June 2025; 20(3): 434-444
Received: 23-11-2024
Peer Reviewed: 08-01-2025
Revised: 05-03-2025
Accepted: 09-03-2025
Published: 17-06-2025

School of Pharmacy & Pharmaceutical Sciences
Isfahan University of Medical Sciences

Original Article

Effect of resveratrol on key signaling pathways including SIRT1/AMPK/Smad3/TGF-β and miRNA-141 related to NAFLD in an animal model

Sahar Yarahmadi[1,2], Mohammadjavad Sotoudeheian[3], Navid Farahmandian[4], Yaser Mohammadi[1], Mehdi Koushki[5], Esmaeel Babaeenezhad[2], Zeynab Yousefi[1], and Soudabeh Fallah[1,*]

[1]*Department of Biochemistry, School of Medicine, Iran University of Medical Sciences, Tehran, I.R. Iran.*
[2]*Nutritional Health Research Center, Lorestan University of Medical Sciences, Khorramabad, I.R. Iran.*
[3]*Physiology Research Center, School of Medicine, Iran University of Medical Sciences, Tehran, I.R. Iran.*
[4]*Department of Tissue Engineering and Regenerative Medicine, School of Advanced Technologies in Medicine, Iran University of Medical Sciences, Tehran, I.R. Iran.*
[5]*Department of Clinical Biochemistry, School of Medicine, Zanjan University of Medical Sciences, Zanjan, I.R. Iran.*

Abstract

Background and purpose: Non-alcoholic fatty liver disease (NAFLD) is a chronic metabolic condition characterized by the accumulation of excess fat in the liver, which can ultimately lead to fibrosis and cirrhosis. This study investigated the impact of resveratrol on the signaling pathways miR-141/SIRT1/AMPK/TGF-β/Smad3 in fatty liver of male C57/BL6 mice.

Experimental approach: Twenty-one male C57/BL6 mice were acclimatized for 10 days and divided into 3 groups (n = 7), including control, NAFLD, and NAFLD + resveratrol groups. After an 8-week HFD to induce NAFLD, the mice were treated with resveratrol (100 mg/kg/day; oral gavage) for 8 weeks. At the end of the study (16 weeks), serum and liver tissue samples were collected. Gene expression was assessed using RT-PCR, while protein levels were analyzed *via* Western blotting. Statistical analysis was performed using SPSS 16.

Findings/Results: The results of the study showed that the expression levels of the genes Smad3 and miRNA-141 were significantly reduced in the resveratrol-treated group compared to the NAFLD group, while the expression levels of SIRT1 and TGF-β were significantly increased. In addition, the Western blot results indicated that the levels of the proteins P-AMPK and SIRT1 in the resveratrol-treated group were significantly higher compared to the NAFLD group. Furthermore, a significant reduction in fat accumulation and degeneration was observed in the histopathological findings of the liver in the resveratrol-treated group.

Conclusion and implications: The study concluded that resveratrol has the potential to reduce liver damage from NAFLD by modulating various signaling pathways, particularly TGF-β/Smad3, SIRT1/AMPK, and miRNA-141, leading to improved lipid metabolism and reduced hepatic steatosis. While the findings underscored the multifaceted therapeutic effects of resveratrol, further research and clinical trials are necessary to fully understand its mechanisms and applications in humans.

Keywords: miRNA-141; Non-alcoholic fatty liver disease; Resveratrol; SIRT1; TGF-β.

INTRODUCTION

Non-alcoholic fatty liver disease (NAFLD) is characterized by lipid metabolism disorders and excessive fat accumulation in liver cells, making it one of the most prevalent chronic liver disorders (1). It is estimated that over 25% of the global population suffers from NAFLD, and its prevalence is increasing in developing countries due to lifestyle changes (2,3).

*Corresponding author: S. Fallah
Tel: +98-2186701, Fax: +98-2188622742
Email: fallah.s@iums.ac.ir, s.fallah13677@gmail.com

Access this article online	
	Website: http://rps.mui.ac.ir
	DOI: 10.4103/RPS.RPS_220_24

NAFLD is also shown to be more prevalent in populations where type 2 diabetes (T2DM), insulin resistance, and obesity are more widespread (4). The spectrum of NAFLD includes simple steatosis, characterized by fat accumulation without inflammation, and non-alcoholic steatohepatitis (NASH), which involves both fat accumulation and inflammation, representing a variety of liver disorders (2,4). In the early stages of NAFLD, due to the increased influx of free fatty acids into the liver, enhanced lipogenesis, and reduced oxidation and disposal of fat, lipotoxicity occurs, leading to oxidative stress, immune system activation, inflammation, and ultimately hepatocyte cell death (5). In advanced stages, the excessive activation of immune cells results in a sustained inflammatory state, pushing the liver toward fibrosis and cirrhosis (5,6).

Studies have identified several factors, including insulin resistance, T2DM, metabolic syndrome, and obesity, as the primary drivers of NAFLD (6). However, the underlying causes of this disease remain elusive. In recent years, special attention has been paid to the molecular pathways involved in NAFLD. Among these, the sirtuin1(SIRT1)/AMP-activated protein kinase (AMPK) and transforming growth factor-β (TGF-β)/Smad3 pathways play critical roles in regulating inflammation and lipid metabolism (7,8). It has been shown that SIRT1 increases fatty acid oxidation and improves insulin sensitivity through the activation of the AMPK pathway (7). Moreover, SIRT1 is recognized as a key regulator of inflammation and oxidative stress (9), while the TGF-β/Smad3 signaling pathway is directly involved in the fibrotic processes of the liver, playing a crucial role in the progression toward fibrosis and cirrhosis (8,10). Chen *et al*. showed that acetylated Smad3 plays a crucial role in tissue fibrosis in dilated cardiomyopathy, whose levels can be increased by TGF-β1 and decreased by activating histone deacetylase, such as Sirt (11). Alongside the signaling pathways, recent studies have highlighted the role of microRNAs (miRNAs) as key regulators of the signaling processes. miRNA-141 is one of the most important miRNAs involved in the regulation of the Smad3/TGF-β and SIRT1/AMPK pathways, and the progression of diseases such as cancer, cardiovascular and liver (12). Wang *et al*. showed that miR-141 down-regulated in endometrial tissues inhibits TGF-β1-induced epithelial-mesenchymal transition and cell invasion, suggesting its potential as a protective factor against endometriosis (13). Previous studies showed that high glucose concentration increases miR-14 levels and decreases SIRT1 mRNA and protein levels, as well as AMPK phosphorylation in HepG2 cells (12). Due to its critical role in NAFLD, miRNA-141 has attracted significant attention from researchers.

Given the severe side effects and irreversible damage caused by chemical drugs, researchers have increasingly turned their focus to natural plant-based treatments such as resveratrol, which is a polyphenolic substance found abundantly in grapes. Previous studies have demonstrated that resveratrol has significant antioxidant and anti-inflammatory effects, largely due to its polyphenolic structure (14). Resveratrol activated SIRT1, which directly bound to Smad3 and promoted its deacetylation, leading to a decrease in collagen type I and III expression in dilated cardiomyopathy (11). Rashidi *et al*. demonstrated that resveratrol reduced fibrosis and steatosis in a model of NAFLD by inhibiting TGF-β-Smad3 metabolism (15).

Despite numerous studies demonstrating the efficacy of resveratrol in modulating various signaling pathways associated with metabolic diseases, there was a clear gap regarding the effect of resveratrol on multiple signaling pathways and the interaction of miRNA-141 in the pathways in the fatty liver model. Given the medicinal effects of resveratrol and the link between miRNA-141 and NAFLD, we were motivated to conduct the present study, aimed at investigating the effects of resveratrol on the expression of SIRT1, AMPK, Smad3, and TGF-β genes and the regulation of miRNA-141 in an animal model of NAFLD.

MATERIALS AND METHODS

Materials

Resveratrol was obtained from Sigma-Aldrich (St Louis, USA). The high-fat diet (HFD), formulated with 60% fat, 20% crude protein, 20% carbohydrate, and an energy

density of 5.21 kcal/g, was purchased from New Jersey (Cat. No. D12492, New Brunswick, NJ, USA). The standard chow diet (SCD), formulated with 6.2% fat, 18% crude protein, 4% crude fiber, 45% carbohydrate, and an energy density of 3.1 kcal/g, was prepared from Madison (Cat. No. Teklad 7013, Madison, WI, USA).

Animals

A total of 21 male C57/BL6 mice (weighing 15-18 g) were purchased from the Laboratory Animal Center (Iran University of Medical Sciences, Tehran, Iran). Animals were kept in a room with a 12-h light/dark cycle, a regulated temperature of 20-26 °C, and a humidity level of 55 ± 5% (Laboratory Animal Center, Iran University of Medical Sciences, Tehran, Iran). Standard laboratory cages were used to acclimate the mice for 10 days. During this period, they had ad libitum access to SCD and water. This study was approved by the Ethics Committee of Iran University of Medical Sciences (Ethical code: IR.IUMS.FMD.REC.1399.065) and conducted according to the animal experimental criteria authorized by the National Institutes of Health in the United States (NIH, 1978).

Experimental design

Following a 10-day period of acclimation, the mice were divided into 3 groups at random (n = 7), using a block randomization method. Group 1 fed with an SCD (control); group 2 fed with an HFD (NAFLD); group 3 fed with an HFD and treated with resveratrol (NAFLD + resveratrol). To induce NAFLD, the animals received the HFD for 8 weeks. After this period, 2 animals were randomly selected and sacrificed to confirm the induction of NAFLD *via* biochemical tests and liver tissue pathology. Once NAFLD was confirmed, the mice were treated with resveratrol at a dose of 100 mg/kg/day *via* oral gavage for 8 weeks (3,16-18). Notably, control and NAFLD groups received normal saline concurrently during the treatment period.

Sample collection

At the end of a 16-week period of study, the animals were deeply anesthetized with a single dose of ketamine (75 mg/kg; intraperitoneally) and xylazine (10 mg/kg; intraperitoneally). Blood samples were collected from the inferior vena cava. To extract the serum, the drawn blood was centrifuged for 10 min at 4 °C and 3000 rpm. The serum samples were then stored at -20 °C for subsequent analysis of the relevant biochemical parameters. Following blood collection, the liver tissues were rapidly excised, rinsed in cold saline, and immediately frozen in liquid nitrogen. The frozen liver samples were then stored at -80 °C for future analyses.

Histopathology of the liver

To maintain tissue morphology, livers were meticulously removed and promptly preserved in 10% neutral-buffered formalin. The samples underwent a 24-h fixation phase before being dehydrated and cleared in xylene using a succession of ethanol solutions with progressively higher concentrations (70%, 80%, 90%, and 100%). Subsequently, paraffin blocks were used to insert the dried tissues. A rotary microtome (Leica RM2235, Leica Microsystems, Germany) was used to cut sections of the paraffin-embedded liver tissues that were 4-5 µm thick. Following their mounting on glass slides and xylene deparaffinization, the thin slices were rehydrated using decreasing ethanol concentrations (100%, 90%, 80%, and 70%) to water. The tissue slices were stained with hematoxylin and eosin in order to evaluate the overall liver architecture and identify any pathological alterations. The liver tissue samples were examined by a veterinary pathologist in a blinded manner. A microscope was used to view the stained slides. This study used the Brunt scoring system or NAFLD/NASH based on the presence of steatosis (fat), ballooning degeneration of hepatocytes, and lobular/portal inflammation, as well as fibrosis. Steatotic hepatocytes contain large lipid vacuoles that displace the nuclei to the periphery of the cells. Ballooning degeneration is characterized by enlarged and swollen hepatocytes with granular material in the cytoplasm, which represents collapsed cytoskeleton (19,20). The grades of steatosis included grade 1 (≤ 33%), grade 2 (33-66%),

and grade 3 (≥ 66%). The degree of lobular inflammation was scored from 0-3 based upon the number of foci that showed lobular inflammation per 20× fields (Table 1). The degree of portal inflammation (Table 2) was assigned as follows: 0 (none), 1 (mild), 2 (moderate), and 3 (marked). Lastly, the fibrosis was staged as follows: 0 (no fibrosis), 1 (perisinusoidal fibrosis), 2 (periportal and perisinusoidal fibrosis), 3 (bridging fibrosis), and 4 (cirrhosis). The final report included the activity grade scored as mild (grade 1), moderate (grade 2), or severe (grade 3) and the stages of fibrosis, including 1-4 (20) (Table 3).

Gene expression analysis

RNA extraction was the first step in the procedure to evaluate gene expression. A homogenizer was used to homogenize 50 mg of frozen liver tissue in liquid nitrogen. TRIzol reagent (Yekta Tajhiz, Iran) was used to extract total RNA in accordance with the manufacturer's instructions. A NanoDrop spectrophotometer (Thermo Scientific, Wilmington, DE, USA) was used to determine the RNA purity, and 1% agarose gel electrophoresis was used to assess the extracted RNA quality and integrity. Following the manufacturer's instructions, high-quality RNA was then reverse-transcribed into complementary DNA (cDNA) using a cDNA synthesis kit (DNAbiotech, Iran).

Using an ABI Step-One system (Applied Biosystems, USA) and a Real Plus 2× Master Mix Green (Amplicon, Denmark), real-time PCR (RT-PCR) was used to measure gene expression. A 10-min initial denaturation at 95 °C was followed by 40 cycles of denaturation at 95 °C for 15 s, annealing at 65 °C for 30 s, and extension at 72 °C for 30 s as part of the PCR amplification process. To standardize gene expression levels, glyceraldehyde 3-phosphate dehydrogenase (GAPDH) was employed as the internal reference gene (21,22). To guarantee accuracy, all RT-PCR reactions were carried out in triplicate, and transcript levels were determined using the delta cycle threshold (ΔCt) technique. Using the $2^{-\Delta\Delta Ct}$ technique, the relative gene expression was determined. Table 4 lists the primer sequences employed in the analysis.

Table 1. Brunt scoring system for NASH.

Grade of activity	Steatosis	Ballooning	Inflammation
Mild, grade 1	1-2 (up to 66%)	Minimal	L = 1-2; P = 0-1
Moderate, grade 2	2-3	Present	L = 1-2; P = 1-2
Severe, grade 3	2-3	Marked	L = 3; P = 1-2

L, Lobular; P, portal.

Table 2. Brunt scoring system for lobular and portal inflammation.

Lobular inflammation		Portal inflammation	
Degree	**Description**	**Degree**	**Description**
0	None	0	None
1	< 2 foci/20 × field	1	Mild
2	2-4/20 × field	2	Moderate
3	> 4/20 × field	3	Marked

Table 3. Brunt scoring system for fibrosis.

Stage of fibrosis	Zone 3 perisinusoidal fibrosis	Periportal fibrosis	Bridging fibrosis	Cirrhosis
1	Focal or extensive	0	0	0
2	As above	Focal or extensive	0	0
3	±	±	+	0
4	±	±	Extensive	+

Table 4. Primer sequences for the real-time PCR method.

Gene	Primer sequence	Primer efficiency
SIRT1	Forward: 5'-TCTGAAAGTGAGACCAGTAGC-3' Reverse: 5'-ATAACATCGCAGTCTCCAAGG-3'	0.95
Smad3	Forward: 5'-TCCAGTCTCCCAACTGCAACC-3' Reverse: 5'-TCGTAGTAGGAGATGGAGCAC-3'	0.91
TGF-β	Forward: 5'-ACGGAATACAGGGCTTTCGAT-3' Reverse: 5'-AGGTAACGCCAGGAATTGTTG-3'	1
GAPDH	Forward: 5'-AGGTTGTCTCCTGCGACT-3' Reverse: 5'-TGCTGTAGCCGTATTCATTGTCA-3'	0.99
miRNA-141-3p	Forward: 5'-GCCGCTAACACTGTCTGGTAA-3' Reverse: 5'-CGTGCAGGGTCCGAGGTA-3'	0.85

TGF-β, Transforming growth factor-β; GAPDH, glyceraldehyde 3-phosphate dehydrogenase.

Western blotting

Liver tissues were lysed using a protease inhibitor cocktail and RIPA buffer to extract cellular proteins. The protein lysates were collected following the manufacturer's protocol (Santa Cruz Biotechnology, USA). The total protein concentration in the samples was quantified using a bicinchoninic acid (BCA) assay kit (Thermo Fisher Scientific, UK). For protein separation, sodium dodecyl sulfate-polyacrylamide gel electrophoresis (SDS-PAGE) was employed, followed by electrotransfer onto a polyvinylidene fluoride (PVDF) membrane (Millipore, USA) at 4 °C for 4 h. To block nonspecific binding sites, the membranes were incubated with appropriate blocking reagents. Specifically, 5% bovine serum albumin (BSA) was used for blocking AMPK, while skim milk in Tris-buffered saline with Tween-20 (TBST) was applied for blocking the SIRT1 protein. After blocking, the membranes were incubated overnight at 4 °C with primary antibodies diluted at 1:1000. The antibodies used included mouse monoclonal anti-SIRT1 (sc-74465), anti-GAPDH (sc-47778), and rabbit polyclonal anti-AMPK (sc-33524), targeting SIRT1, AMPK, and GAPDH, respectively.

Following the primary antibody incubation, the membranes were washed 3 times with TBST (0.05% Tween-20 in Tris-NaCl buffer) to remove any unbound antibodies. The membranes were then incubated with the secondary antibody, HRP-conjugated anti-IgG (sc-2357), at room temperature for 3 h. After 3 additional washes with TBST, the proteins were visualized using enhanced chemiluminescence (ECL) substrate (Amersham, USA) and a Western blotting imaging system. The intensity of the protein bands was analyzed using ImageJ software (NIH, Bethesda, USA), allowing for the quantification of relative protein expression levels. GAPDH served as the internal loading control to ensure accurate normalization of protein levels across samples.

Statistical analysis

Data were shown as mean ± standard deviation (SD) and analyzed by SPSS Statistics version 16.0 (Chicago, USA). The Shapiro-Wilk test was used to determine if the data distribution was normal. Analysis of variance (ANOVA) followed by a Tukey post-hoc test was used to compare groups if the normality assumption was met. Non-parametric options, including the Kruskal-Wallis or Wilcoxon tests, were used when the normality assumption was broken. P-value $\leq$ 0.05 was considered statistically significant.

RESULTS

Effect of resveratrol on the liver histopathological changes

Figure 1 illustrates the histopathological changes in the liver tissue across the studied groups. As observed, the liver tissue of the mice in the control group appeared completely normal, with no detectable abnormalities (Fig. 1A). In contrast, the liver tissue of mice in the NAFLD group exhibited significant pathological changes, including lipid-laden hepatocytes, severely degenerated cells, and nuclei displaced toward the cytoplasmic wall,

confirming the successful induction of NAFLD (Fig. 1B). However, the histopathological alterations, including degenerated cells, fat-laden hepatocytes, and displaced nuclei, were significantly reduced in the NAFLD + RSV group compared with the NAFLD group, with the liver tissue resembling the control group to a notable extent (Fig. 1C).

Effect of resveratrol on relative gene expression

Figure 2 depicts the relative changes in the expression of the genes SIRT1, Smad3, TGF-β, and miRNA-141 across the studied groups. The results indicated an increase in the relative expression of miRNA-141 (1.24-fold) and Smad3 (1.99-fold) in the NAFLD group compared with the control group (Fig. 2A and C), while the expression of SIRT1 was significantly reduced (4.55-fold) (Fig. 2B). Furthermore, the relative expression of miRNA-141 (2.33-fold) and Smad3 (1.53-fold) was significantly decreased in the resveratrol-treated group compared with the NAFLD group (Fig. 2A and C), whereas the expression of SIRT1 (3.32-fold) and TGF-β (4.69-fold) was markedly upregulated in the group receiving resveratrol in comparison to NAFLD group (Figs. S1 and 2B and D).

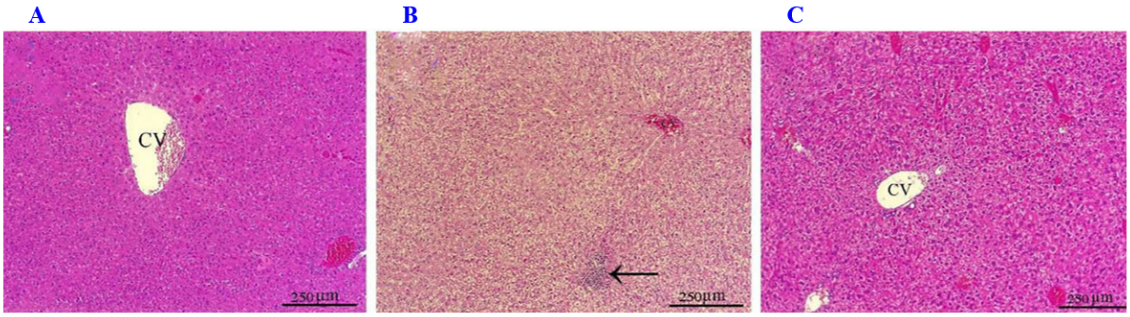

Fig. 1. NAFLD-induced histopathological changes in liver tissues in experimental groups. (A) Control group with normal liver structure; (B) NAFLD group, the lipid-laden hepatocytes were thoroughly degenerated. Most nuclei were pushed toward the cytoplasmic wall; (C) NAFLD + resveratrol group, the hepatocytes were very similar to normal hepatocytes with minimal changes in their structures. The nuclei were located in a normal position compared to fatty liver hepatocytes. The liver tissues were stained with hematoxylin and eosin. The NAFLD model was induced by receiving a high-fat diet for 8 weeks. Resveratrol was administered at a dose of 100 mg/kg/day *via* oral gavage for 8 weeks. Control and NAFLD groups received normal saline concurrently during the treatment period. NAFLD, non-alcoholic fatty liver disease; CV, central vein.

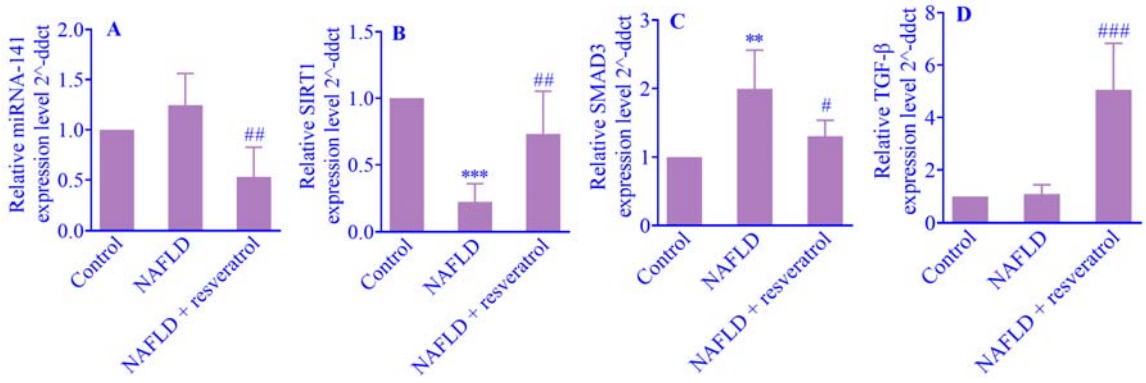

Fig. 2. The expression level of genes in the experimental groups. Relative expression of (A) miRNA-141; (B) SIRT1; (C) SMAD3; (D) TGF-β. The NAFLD model was induced by receiving a high-fat diet for 8 weeks. Resveratrol was administered at a dose of 100 mg/kg/day *via* oral gavage for 8 weeks. Control and NAFLD groups received normal saline concurrently during the treatment period. Data were reported as mean ± SD. $^{*}P < 0.05$, $^{**}P < 0.01$, and $^{***}P < 0.001$ indicate significant differences compared with the control group; $^{\#}P < 0.05$, $^{\#\#}P < 0.01$, and $^{\#\#\#}P < 0.001$ versus NAFLD group. NAFLD, non-alcoholic fatty liver disease; miR-141, miRNA141; SIRT1, sirtuin1; TGF-β, transforming growth factor-β.

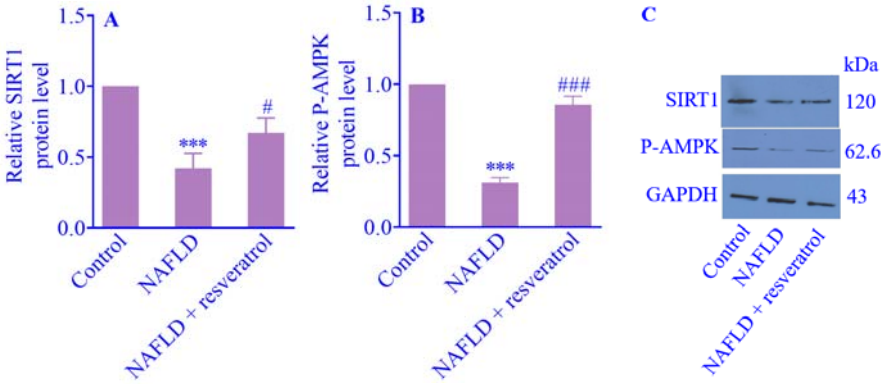

Fig. 3. The levels of SIRT1 and P-AMPK proteins in the experimental groups. (A) SIRT1 protein level; (B) P-AMPK protein level; (C) Western blot bands of SIRT1 and P-AMPK proteins. The NAFLD model was induced by receiving a high-fat diet for 8 weeks. Resveratrol was administered at a dose of 100 mg/kg/day *via* oral gavage for 8 weeks. Control and NAFLD groups received normal saline concurrently during the treatment period. Data were reported as mean ± SD. $^{***}P < 0.001$ indicates significant difference compared with the control group; $^{\#}P < 0.05$ and $^{\#\#\#}P < 0.001$ versus NAFLD group. NAFLD, non-alcoholic fatty liver disease; miR-141, miRNA-141; GAPDH, Glyceraldehyde 3-phosphate dehydrogenase; SIRT1, Sirtuin1.

Effect of resveratrol on the SIRT1/AMPK protein level

Figure 3 depicts the protein levels of AMPK and SIRT1 in the experimental groups. The protein levels of SIRT1 (2.38%) and P-AMPK (3.22%) were significantly decreased in the NAFLD group compared with the control group (Fig. 3A and B). However, treatment with resveratrol 100 mg/kg significantly increased the levels of SIRT1 (1.59-fold) and P-AMPK (2.76-fold) compared with the NAFLD group (Fig. 3A and B). Figures 3C and S2 exhibit Western blot bands of SIRT1 and P-AMPK protein levels in the experimental groups.

DISCUSSION

The current study investigated for the first time the multiple signaling pathways modulated by resveratrol, elucidated the miRNA interactions and developed a comprehensive therapeutic profile that includes antioxidant and anti-inflammatory responses. As this study warrants further investigation into the underlying mechanisms and clinical translation of resveratrol, it lays a solid foundation for future research ambitiously aiming to redefine the treatment of NAFLD. Overall, the results demonstrated that resveratrol could significantly prevent the changes induced by NAFLD conditions, including histopathological liver alterations, gene expression changes, and protein levels. The results suggested that resveratrol could play an important role in improving NAFLD conditions.

It has been shown that SIRT1 plays a crucial role as a key regulator in glucose and lipid metabolism (23). SIRT1 increases the sensitivity of hepatocytes to insulin (24). The results of the present study indicated that the expression of SIRT1 was significantly reduced in the NAFLD group compared with the control group. Therefore, a reduction in SIRT1 is associated with the accumulation of fat in hepatocytes and the exacerbation of hepatic steatosis (25), which aligns with the histopathological findings of this study. In the resveratrol-treated group, the expression of SIRT1 considerably increased compared to the NAFLD group, indicating the protective effect of resveratrol. Ajmo *et al*. determined that administering resveratrol significantly elevates SIRT1 levels in the livers of mice subjected to ethanol, counteracting the reductions typically observed in conditions of hepatic steatosis (26). Additionally, it has been shown that SIRT1 affects fat metabolism through the activation of AMPK (27). When activated, AMPK inhibits lipogenesis by directly phosphorylating and inactivating acetyl-CoA carboxylase and hormone-sensitive lipase. The actions lead to a reduction in fatty acid synthesis and an increase in fat oxidation, promoting the breakdown of stored lipids as an energy source (27). AMPK, as a cellular energy sensor, reduces lipogenesis and increases lipolysis, thereby decreasing liver triglyceride levels and preventing the

progression of NAFLD (9,28,29). In this study, the levels of the P-AMPK protein also decreased in the NAFLD group, which was consistent with the reduced expression of SIRT1. However, treatment with resveratrol significantly increased the levels of P-AMPK in the treated group. Similarly, Alberdi *et al.* showed that resveratrol treatment in HFD-fed rats resulted in a significant increase in hepatic AMPK phosphorylation, which consequently improved liver function and reduced lipid accumulation in the liver (30). Overall, the outcomes suggested that resveratrol may reduce NAFLD-related damage, including hepatic steatosis, through the SIRT1/AMPK pathway (31).

The TGF-β/Smad3 pathway is one of the key pathways in the progression of liver fibrosis (15). The present study results showed that the expression of miRNA-141 and Smad3 was markedly increased in the NAFLD group, indicating increased liver damage and the progression of liver fibrosis, which is consistent with the histopathological findings.

miRNA-141 targets SIRT1, a key regulator of lipid metabolism, leading to fat accumulation in hepatocytes and the progression of NAFLD (12). Thus, miRNA-141 exerts its negative effects by down-regulating SIRT1 (12). However, Smad3, a key player in the TGF-β/Smad3 pathway, plays a role in the development of liver fibrosis linked to NAFLD (32,33). In this study, the increased expression of miRNA-141 and Smad3 in the NAFLD group aligned with the mechanisms, showing that the pathways play a key role in disease progression. Yamaguchi *et al*. showed that SMAD3 interactions with other signaling pathways can either promote hepatocyte protection or contribute to liver injury (34). In the resveratrol-treated group, the significant decrease in Smad3 and miRNA-141 indicated that resveratrol could inhibit the harmful pathways. The reduction in miRNA-141 suggested an increase in SIRT1 (12), which ultimately reduces the accumulation of fat in the liver and improves the condition of NAFLD. Furthermore, the reduction in Smad3 indicates that resveratrol inhibited the TGF-β/Smad3 pathway, potentially reducing liver fibrosis (15). These findings align with other studies (10,15,35).

While it was expected that the expression of TGF-β would decrease in the resveratrol-treated group, similar to Smad3, it significantly increased. Although this might initially seem contradictory, the increased expression of TGF-β could be part of a compensatory or protective response (36). It has been shown that TGF-β can play a dual role (37). On one hand, it is involved in inflammation and fibrosis , and on the other hand, it plays a role in tissue repair and regeneration (38). Following tissue damage, TGF-β is activated from its latent form and secreted into the extracellular environment, promoting the recruitment and activation of various cell types, including fibroblasts, macrophages, and endothelial cells (39). Upon binding to its receptors, TGF-β initiates a cascade of intracellular signaling pathways that lead to the production of extracellular matrix (ECM) proteins, such as collagen, which are crucial for tissue repair and integrity. The ECM remodeling is fundamental in restoring tissue architecture and function following injury (40,41). On the other hand, the TGF-β signaling pathway is highly complex and multifaceted (42), and it is possible that resveratrol, by modulating downstream pathways of TGF-β, increases its positive effects, such as liver tissue repair and regeneration (14,15,43,44), which is consistent with the liver histopathological results.

The histopathological findings of the liver tissues indicated that the HFD used in this study successfully induced NAFLD in animals (45-47). Additionally, the protective effects of resveratrol in reducing the liver damage caused by NAFLD were observed. The present results showed that fat accumulation and cellular degeneration significantly decreased in the resveratrol-treated group. As mentioned earlier, the effects of resveratrol might be due to its impact on the SIRT1/AMPK (9), and TGF-β/Smad3 signaling pathways (36,48), as well as the reduced expression of miRNA-141 (49,50), which was discussed in detail. Furthermore, resveratrol, as a polyphenolic compound with antioxidant and anti-inflammatory properties, may exert its protective effects on liver tissue (16,51).

This study had several strengths. I. The successful induction of NAFLD and observation of histopathological changes in liver tissue confirmed the accuracy of the modeling; II. the simultaneous investigation of

multiple signaling pathways associated with NAFLD; III. the evaluation of miRNA-141 as a key regulator in the examined signaling pathways. Despite the best efforts, the present study had limitations, including I. the lack of assessment of all key protein levels; II. the evaluation of the short-term effects of resveratrol on NAFLD, thus requiring long-term studies; III. the focuses on certain key signaling pathways related to NAFLD, while the investigation of other related pathways, such as oxidative stress and inflammation (e.g., peroxisome proliferator-activated receptors or nuclear factor kappa-light-chain-enhancer of activated B cells), which play significant roles in NAFLD, is important; IV. the absence of clinical evaluations, as this study was conducted in the animal phase, necessitating clinical trials for generalization to humans.

CONCLUSION

The results of this study indicated that resveratrol could act as a potential therapeutic agent in reducing the liver damage caused by NAFLD. Resveratrol exerts its protective effects through multiple signaling pathways, including TGF-β/Smad3 and SIRT1/AMPK. By increasing SIRT1 expression and activating AMPK, resveratrol could reduce hepatic steatosis, improve lipid metabolism, and ultimately prevent the progression of NAFLD. Additionally, it was shown that the downregulation of miRNA-141 led to the regulation of related signaling pathways. These findings highlighted the multifaceted effects of resveratrol as a natural polyphenolic compound with antioxidant and anti-inflammatory properties, emphasizing its significant role in modulating the signaling pathways associated with NAFLD. However, further study is needed to clarify the mechanisms of resveratrol, and clinical trials are required for human application. Overall, future research should focus on further elucidating the therapeutic potential and underlying mechanisms of resveratrol for treating NAFLD.

Acknowledgments

All authors would like to thank everyone who cooperated with us on this project, including the employees in the Center of Experimental Studies and Laboratory Animals, Iran University of Medical Sciences. This research was financially supported by the Iran University of Medical Sciences (Grant No. 19462).

Conflict of interest statement

The authors declared no conflict of interest in this study.

Authors' contributions

S. Fallah, S. Yarahmadi, M. Sotoudeheian, Y. Mohammadi, and N. Farahmandian contributed to the study conception and design, data preparation and analysis, and writing and editing the manuscript; E. Babaeenezhad, Y. Mohammadi, Z. Yousefi, and M. Koushki participated in the research and writing and editing of the manuscript. All authors have read and approved the final version of the manuscript.

Supplementary materials

The supplementary materials for this article can be found online at: https://github.com/yasermohammadi73/supplementary

REFERENCES

1. Babaeenezhad E, Farahmandian N, Sotoudeheian M, Dezfoulian O, Askari E, Taghipour N, *et al*. Resveratrol relieves hepatic steatosis and enhances the effects of atorvastatin in a mouse model of NAFLD by regulating the renin-angiotensin system, oxidative stress, and inflammation. Food Sci Nutr. 2025;13(3):e70073,1-12. DOI: 10.1002/fsn3.70073.
2. Lee ECZ, Anand VV, Razavi AC, Alebna PL, Muthiah MD, Siddiqui MS, *et al*. The global epidemic of metabolic fatty liver disease. Curr Cardiol Rep. 2024;26(4):199-210. DOI: 10.1007/s11886-024-02025-6.
3. Yarahmadi S, Farahmandian N, Fadaei R, Koushki M, Bahreini E, Karima S, *et al*. Therapeutic potential of resveratrol and atorvastatin following high-fat diet uptake-induced nonalcoholic fatty liver disease by targeting genes involved in cholesterol metabolism and miR33. DNA Cell Biol. 2023;42(2):82-90. DOI: 10.1089/dna.2022.0581.
4. Kuchay MS, Choudhary NS, Mishra SK. Pathophysiological mechanisms underlying MAFLD. Diabetes Metab Syndr. 2020;14(6):1875-1887. DOI: 10.1016/j.dsx.2020.09.026.
5. Benedict M, Zhang X. Non-alcoholic fatty liver disease: an expanded review. World J Hepatol. 2017;9(16):715-732. DOI: 10.4254/wjh.v9.i16.715.
6. Nassir F. NAFLD: mechanisms, treatments, and biomarkers. Biomolecules. 2022;12(6):824,1-32. DOI: 10.3390/biom12060824.

7. Wu Y, Liu X, Zhou Q, Huang C, Meng X, Xu F, *et al*. Silent information regulator 1 (SIRT1) ameliorates liver fibrosis *via* promoting activated stellate cell apoptosis and reversion. Toxicol Appl Pharmacol. 2015;289(2):163-176. DOI: 10.1016/j.taap.2015.09.028.
8. Yadav H, Devalaraja S, Chung ST, Rane SG. TGF-β1/Smad3 pathway targets PP2A-AMPK-FoxO1 signaling to regulate hepatic gluconeogenesis. J Biol Chem. 2017;292(8):3420-3432. DOI: 10.1074/jbc.M116.764910.
9. Price NL, Gomes AP, Ling AJ, Duarte FV, Martin-Montalvo A, North BJ, *et al*. SIRT1 is required for AMPK activation and the beneficial effects of resveratrol on mitochondrial function. Cell Metab. 2012;15(5):675-690. DOI: 10.1016/j.cmet.2012.04.003.
10. He H, Zhong Y, Wang H, Tang PMK, Xue VW, Chen X, *et al*. Smad3 mediates diabetic dyslipidemia and fatty liver in db/db mice by targeting PPARδ. Int J Mol Sci. 2023;24(14):11396,1-19. DOI: 10.3390/ijms241411396.
11. Chen Q, Zeng Y, Yang X, Wu Y, Zhang S, Huang S, *et al*. Resveratrol ameliorates myocardial fibrosis by regulating Sirt1/Smad3 deacetylation pathway in rat model with dilated cardiomyopathy. BMC Cardiovasc Disord. 2022;22(1):17,1-10. DOI: 10.1186/s12872-021-02401-y.
12. Yousefi Z, Nourbakhsh M, Abdolvahabi Z, Ghorbanhosseini SS, Hesari Z, Yarahmadi S, *et al*. microRNA-141 is associated with hepatic steatosis by downregulating the sirtuin1/AMP-activated protein kinase pathway in hepatocytes. J Cell Physiol. 2020;235(2):880-890. DOI: 10.1002/jcp.29002.
13. Wang S, Zhang M, Zhang T, Deng J, Xia X, Fang X. microRNA-141 inhibits TGF-β1-induced epithelial-to-mesenchymal transition through inhibition of the TGF-β1/SMAD2 signaling pathway in endometriosis. Arch Gynecol Obstet. 2020;301(3):707-714. DOI: 10.1007/s00404-019-05429-w.
14. Faghihzadeh F, Hekmatdoost A, Adibi P. Resveratrol and liver: a systematic review. J Res Med Sci. 2015;20(8):797-810. DOI: 10.4103/1735-1995.168405.
15. Rashidi M, Afarin R, Kouchak M, Kabizadeh B, Shamsi M, Hatami M. Resveratrol and Saroglitazar: a promising combination for targeting TGF-β/Smad3 signaling and attenuating inflammatory response in nonalcoholic steatohepatitis in rats. Hepat Mon. 2023;23(1):1-12. DOI: 10.5812/hepatmon-138237.
16. Heebøll S, Thomsen KL, Pedersen SB, Vilstrup H, George J, Grønbæk H. Effects of resveratrol in experimental and clinical non-alcoholic fatty liver disease. World J Hepatol. 2014;6(4):188-198. DOI: 10.4254/wjh.v6.i4.188.
17. Cheng K, Song Z, Zhang H, Li S, Wang C, Zhang L, *et al*. The therapeutic effects of resveratrol on hepatic steatosis in high-fat diet-induced obese mice by improving oxidative stress, inflammation and lipid-related gene transcriptional expression. Med Mol Morphol. 2019;52(4):187-197. DOI: 10.1007/s00795-019-00216-7.
18. Shang J, Chen LL, Xiao FX, Sun H, Ding HC, Xiao H. Resveratrol improves non-alcoholic fatty liver disease by activating AMP-activated protein kinase. Acta Pharmacol Sin. 2008;29(6):698-706. DOI: 10.1111/j.1745-7254.2008.00807.x.
19. Vyas M, Jain D. A practical diagnostic approach to hepatic masses. Indian J Pathol Microbiol. 2018;61(1):2-17. DOI: 10.4103/IJPM.IJPM_578_17.
20. Brunt EM. Nonalcoholic fatty liver disease: pros and cons of histologic systems of evaluation. Int J Mol Sci. 2016;17(1):97,1-10. DOI: 10.3390/ijms17010097.
21. Triki T, Boussora F, Drine S, Ali SB, Gasmi A, Marzougui LBN, *et al*. Stability analysis of reference genes for qPCR studies in *Chenopodium quinoa* ecotypes on salt-affected soils. Pol J Environ Stud. 2024;33(3):2823-2930. DOI: 10.15244/pjoes/172082.
22. Ho KH, Patrizi A. Assessment of common housekeeping genes as reference for gene expression studies using RT-qPCR in mouse choroid plexus. Sci Rep. 2021;11(1):3278,1-15. DOI: 10.1038/s41598-021-82800-5.
23. Nikroo H, Hosseini SRA, Fathi M, Sardar MA, Khazaei M. The effect of aerobic, resistance, and combined training on PPAR-α, SIRT1 gene expression, and insulin resistance in high-fat diet-induced NAFLD male rats. Physiol Behav. 2020;227:113149,1-7. DOI: 10.1016/j.physbeh.2020.113149.
24. Purushotham A, Schug TT, Xu Q, Surapureddi S, Guo X, Li X. Hepatocyte-specific deletion of SIRT1 alters fatty acid metabolism and results in hepatic steatosis and inflammation. Cell Metab. 2009;9(4):327-338. DOI: 10.1016/j.cmet.2009.02.006.
25. Eades G, Yao Y, Yang M, Zhang Y, Chumsri S, Zhou Q. miR-200a regulates SIRT1 expression and epithelial to mesenchymal transition (EMT)-like transformation in mammary epithelial cells. J Biol Chem. 2011;286(29):25992-26002. DOI: 10.1074/jbc.M111.229401.
26. Ajmo JM, Liang X, Rogers CQ, Pennock B, You M. Resveratrol alleviates alcoholic fatty liver in mice. Am J Physiol Gastrointest Liver Physiol. 2008;295(4):G833-G842. DOI: 10.1152/ajpgi.90358.2008.
27. Hu LK, Chen JQ, Zheng H, Tao YP, Yang Y, Xu XF. MicroRNA-506-3p targets SIRT1 and suppresses AMPK pathway activation to promote hepatic steatosis. Exp Ther Med. 2021;22(6):1430,1-8. DOI: 10.3892/etm.2021.10865.
28. Ke W, Huang J, Zhong Y, Shi Y, Yan F, Huang D, *et al*. Hydroxypropyl-beta-cyclodextrin embedded resveratrol regulates gut microbiota to prevent NAFLD *via* activating AMPK signaling pathway. Food Biosci. 2023;54:102907. DOI: 10.1016/j.fbio.2023.102907.

29. Zang M, Xu S, Maitland-Toolan KA, Zuccollo A, Hou X, Jiang B, *et al*. Polyphenols stimulate AMP-activated protein kinase, lower lipids, and inhibit accelerated atherosclerosis in diabetic LDL receptor-deficient mice. Diabetes. 2006;55(8):2180-2191. DOI: 10.2337/db05-1188.
30. Alberdi G, Rodríguez VM, Macarulla MT, Miranda J, Churruca I, Portillo MP. Hepatic lipid metabolic pathways modified by resveratrol in rats fed an obesogenic diet. Nutrition. 2013;29(3):562-567. DOI: 10.1016/j.nut.2012.09.011.
31. Tian Y, Ma J, Wang W, Zhang L, Xu J, Wang K, *et al*. Resveratrol supplement inhibited the NF-κB inflammation pathway through activating AMPKα-SIRT1 pathway in mice with fatty liver. Mol Cell Biochem. 2016;422(1-2):75-84. DOI: 10.1007/s11010-016-2807-x.
32. Ahmed H, Umar MI, Imran S, Javaid F, Syed SK, Riaz R, *et al*. TGF-β1 signaling can worsen NAFLD with liver fibrosis backdrop. Exp Mol Pathol. 2022;124. DOI: 10.1016/j.yexmp.2021.104733.
33. Nair B, Nath LR. Inevitable role of TGF-β1 in progression of nonalcoholic fatty liver disease. J Recept Signal Transduct Res. 2020;40(3):195-200. DOI: 10.1080/10799893.2020.1726952.
34. Yamaguchi T, Yoshida K, Murata M, Suwa K, Tsuneyama K, Matsuzaki K, *et al*. Smad3 phospho-isoform signaling in nonalcoholic steatohepatitis. Int J Mol Sci. 2022;23(11):1-18. DOI: 10.3390/ijms23116270.
35. He H, Wang H, Chen X, Zhong Y, Huang XR, Ma RC, *et al*. Treatment for type 2 diabetes and diabetic nephropathy by targeting Smad3 signaling. Int J Biol Sci. 2024;20(1):200-217. DOI: 10.7150/ijbs.87820.
36. Liu J, Zhuo X, Liu W, Wan Z, Liang X, Gao S, *et al*. Resveratrol inhibits high glucose induced collagen upregulation in cardiac fibroblasts through regulating TGF-β1-Smad3 signaling pathway. Chem Biol Interact. 2015:227:45-52. DOI: 10.1016/j.cbi.2014.12.031.
37. Lim JY, Oh MA, Kim WH, Sohn HY, Park SI. AMP-activated protein kinase inhibits TGF-β-induced fibrogenic responses of hepatic stellate cells by targeting transcriptional coactivator p300. J Cell Physiol. 2012;227(3):1081-1089. DOI: 10.1002/jcp.22824.
38. Budi EH, Schaub JR, Decaris M, Turner S, Derynck R. TGF-β as a driver of fibrosis: physiological roles and therapeutic opportunities. J Pathol. 2021;254(4):358-373. DOI: 10.1002/path.5680.
39. Deng Z, Fan T, Xiao C, Tian H, Zheng Y, Li C, *et al*. TGF-β signaling in health, disease, and therapeutics. Signal Transduct Target Ther. 2024;9(1):61,1-40. DOI: 10.1038/s41392-024-01764-w.
40. Roberts AB, McCune BK, Sporn MB. TGF-beta: regulation of extracellular matrix. Kidney Int. 1992;41(3):557-559. DOI: 10.1038/ki.1992.81.
41. Schiller M, Javelaud D, Mauviel A. TGF-beta-induced SMAD signaling and gene regulation: consequences for extracellular matrix remodeling and wound healing. J Dermatol Sci. 2004; 35(2):83-92. DOI: 10.1016/j.jdermsci.2003.12.006.
42. Aashaq S, Batool A, Mir SA, Beigh MA, Andrabi KI, Shah ZA. TGF-β signaling: a recap of SMAD-independent and SMAD-dependent pathways. J Cell Physiol. 2022;237(1):59-85. DOI: 10.1002/jcp.30529.
43. Silva KAS, Freitas DF, Borém LMA, Oliveira LP, Oliveira JR, Paraíso AF, *et al*. Resveratrol attenuates non-alcoholic fatty liver disease in obese mice modulating MAF1. Revista Brasileira de Farmacognosia. 2022:1-10. DOI:10.1007/s43450-022-00309-y.
44. Li J, Qu X, Ricardo SD, Bertram JF, Nikolic-Paterson DJ. Resveratrol inhibits renal fibrosis in the obstructed kidney: potential role in deacetylation of Smad3. Am J Pathol. 2010;177(3):1065-1071. DOI: 10.2353/ajpath.2010.090923.
45. Andrade JMO, Paraíso AF, de Oliveira MVM, Martins AME, Neto JF, Guimarães ALS, *et al*. Resveratrol attenuates hepatic steatosis in high-fat fed mice by decreasing lipogenesis and inflammation. Nutrition. 2014;30(7-8):915-919. DOI: 10.1016/j.nut.2013.11.016.
46. El-Lakkany NM, Seif El-Din SH, Abdel-Aal Sabra AN, Hammam OA, Abdel-Latif Ebeid F. Co-administration of metformin and N-acetylcysteine with dietary control improves the biochemical and histological manifestations in rats with non-alcoholic fatty liver. Res Pharm Sci. 2016; 11(5):374-382. DOI: 10.4103/1735-5362.192487.
47. Hamidi-Zad Z, Moslehi A, Rastegarpanah M. Attenuating effects of allantoin on the oxidative stress in a mouse model of nonalcoholic steatohepatitis: role of Sirt1/NRF2 Pathway. Res Pharm Sci, 2021;16(6):651-659. DOI: 10.4103/1735-5362.327511.
48. ShamsEldeen AM, Al-Ani B, Ebrahim HA, Rashed L, Badr AM, Attia A, *et al*. Resveratrol suppresses cholestasis-induced liver injury and fibrosis in rats associated with the inhibition of TGFβ1-Smad3-miR21 axis and profibrogenic and hepatic injury biomarkers. Clin Exp Pharmacol Physiol. 2021;48(10):1402-1411. DOI: 10.1111/1440-1681.13546.
49. Huang Y, Tong J, He F, Yu X, Fan L, Hu J, *et al*. miR-141 regulates TGF-β1-induced epithelial-mesenchymal transition through repression of HIPK2 expression in renal tubular epithelial cells. Int J Mol Med. 2015;35(2):311-318. DOI: 10.3892/ijmm.2014.2008.
50. Liang H, Wang X, Si C, Duan Y, Chen B, Liang H, *et al*. Downregulation of miR-141 deactivates hepatic stellate cells by targeting the PTEN/AKT/mTOR pathway. Int J Mol Med. 2020;46(1):406-414. DOI: 10.3892/ijmm.2020.4578.
51. Kisková T, Kassayová M. Resveratrol action on lipid metabolism in cancer. Int J Mol Sci. 2019;20(11):2704,1-20. DOI: 10.3390/ijms20112704.